Bioorganic & Medicinal Chemistry Letters 22 (2012) 3884–3889

Contents lists available at SciVerse ScienceDirect

Bioorganic & Medicinal Chemistry Letters

journal homepage: www.elsevier.com/locate/bmcl

N-Methyl-3-(tetrahydro-2*H*-pyran-4-yl)-2,3,4,9-tetrahydro-1*H*-carbazole-6-carboxamides as a novel class of cannabinoid receptors agonists with low CNS penetration

Zhongyong Wei [a], Hua Yang [a], Ziping Liu [a], Maxime Tremblay [a], Shawn Johnstone [a], Sara Béha [a], Shi Yi Yue [a], Sanjay Srivastava [a], Miroslaw J. Tomaszewski [a], William Brown [a], Christopher Walpole [a], Stéphane St-Onge [b], Etienne Lessard [c], Anne-Julie Archambault [d], Thierry Groblewski [b], Daniel Pagé [a,*]

[a] Department of Medicinal Chemistry, AstraZeneca R&D Montreal, 7171 Frederick-Banting, Saint-Laurent, Quebec, Canada H4S 1Z9
[b] Department of Molecular Pharmacology, AstraZeneca R&D Montreal, 7171 Frederick-Banting, Saint-Laurent, Quebec, Canada H4S 1Z9
[c] Department of DMPK, AstraZeneca R&D Montreal, 7171 Frederick-Banting, Saint-Laurent, Quebec, Canada H4S 1Z9
[d] Department of Bioscience, AstraZeneca R&D Montreal, 7171 Frederick-Banting, Saint-Laurent, Quebec, Canada H4S 1Z9

ARTICLE INFO

Article history:
Received 30 March 2012
Revised 24 April 2012
Accepted 27 April 2012
Available online 4 May 2012

Keywords:
Cannabinoid
Tetrahydrocarbazoles
Pain

ABSTRACT

Cannabinoid CB_1 receptor agonists exhibit potent analgesic effects in rodents and humans, but their clinical utility as analgesic drugs is often limited by centrally mediated side effects. We report herein the preparation of *N*-methyl-3-(tetrahydro-2*H*-pyran-4-yl)-2,3,4,9-tetrahydro-1*H*-carbazole-6-carboxamides as a novel class of hCB_1/hCB_2 dual agonists with attractive physicochemical properties. More specifically, (*R*)-*N*,9-dimethyl-*N*-(4-(methylamino)-4-oxobutyl)-3-(tetrahydro-2*H*-pyran-4-yl)-2,3,4,9-tetrahydro-1*H*-carbazole-6-carboxamide, displayed an extremely low level of CNS penetration (Rat Cbr/Cplasma = 0.005 or 0.5%) and was devoid of CNS side effects during pharmaco-dynamic testing.

Cannabinoid receptors belong to the super family of G-protein coupled receptors (GPCRs) and two of them have been cloned and characterized so far; CB_1 and CB_2.[1,2] CB_1 is widely expressed in neurons in the brain[3,4] and is responsible for most of the psychoactive properties of cannabinoids. Even though it was recently demonstrated that CB_2 is expressed in the central nervous system (CNS) under certain conditions,[5] it is primarily abundant in splenocytes and leukocytes[2] and responsible for many of the immunomodulatory and anti-inflammatory effects of cannabis.[6] CB_1 is also found in a variety of tissues including immune cells. A wide variety of potential therapeutic applications associated with cannabinoid ligands are currently under investigations, including eating disorders,[7] obesity,[8] drug addictions[9] and central immune functions.[5]

Cannabinoids and cannabinoid receptors have been implicated in pain transduction and perception[10] as well as neuroinflammation.[11] Many published studies have demonstrated that cannabinoids, both CB_1 and CB_2 agonists, are potent analgesics not only in a variety of preclinical pain models but also in the clinic.[12–15] Unfortunately, the exploitation of the therapeutic potential of CB_1 agonists in man has been generally limited by their CNS side effects, mostly associated with the CB_1 receptors.[16] Several studies have established that CB_2-selective agonists (relative to CB_1) exhibit efficacy in many rodent pain models and lack the CB_1-mediated

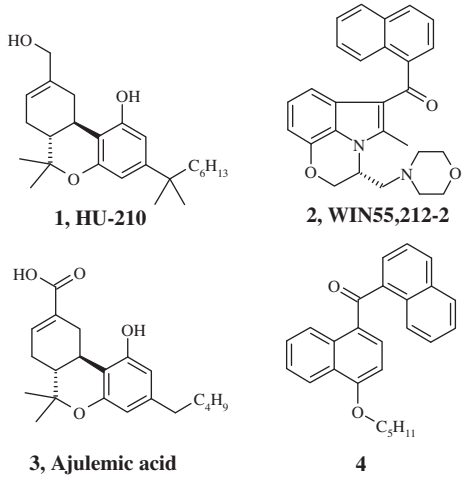

Figure 1. Several CB_1 or CB_1/CB_2 dual agonists.

* Corresponding author. Tel.: +1 514 832 3200; fax: +1 514 832 3232.
E-mail address: daniel.page@astrazeneca.com (D. Pagé).

0960-894X/$ - see front matter © 2012 Elsevier Ltd. All rights reserved.
http://dx.doi.org/10.1016/j.bmcl.2012.04.128

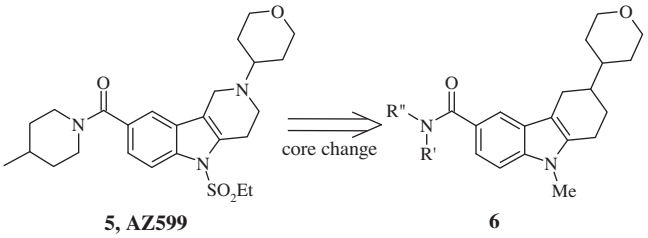

Figure 2. Scaffold-hopping around the γ-carboline core.

CNS effects at analgesic doses.[17,18] Specifically, CB_2-selective agonists have shown efficacy in preclinical models of neuropathic and inflammatory pain.[19,20]

Another approach to effective and safe cannabinoid analgesics would be to aim for the development of low brain penetrant CB_1 agonists[21–26] as analgesic drugs. This strategy, adopted by other groups,[25,26] demonstrated the reduction of CNS side effects by peripherally restricted CB_1 agonists while keeping their analgesic effects. In clinical trials, topical administration of HU-210 (**1**, **Fig. 1**) (a dual CB_1/CB_2 agonist) reportedly reduced thermal and mechanical hyperalgesia and allodynia induced by capsaicin. No psychoactive effects were observed.[27] Ajulemic acid (**3**, **Fig. 1**), a dimethylheptyl analogue of the 11-carboxylic acid metabolite of THC with modest CB_1/CB_2 binding affinity, reportedly has a reduced CNS penetration and showed promising efficacy and a better side effect profile in both animals and humans when compared to Δ9-THC.[28,23] Naphthalen-1-yl-(4-pentyloxynaphthalen-1-yl) methanone (**4, Fig. 1**) was reported to be a CB_1/CB_2 dual agonist[29] with limited brain penetration, displaying good oral bioavailability and potent antihyperalgesic activity in animal models. However, this compound possesses poor physicochemical properties, including an extremely poor solubility.

Our interest in the discovery and development of novel therapeutics for pain management prompted a high-throughput screen of our GPCR focused libraries. The γ-carboline scaffold was identified in the efforts as a chemical series with attractive physicochemical properties.[30] Compound (**5**) (**AZ599**) exhibited binding affinities on both human cannabinoid receptors (hCB_1 *Ki*: 120 nM; hCB_2 *Ki*: 9 nM) and was a CB_1 full agonist (EC_{50}: 49 nM, E_{max}: 120%) with good solubility (>1000 μM) and low CNS penetration (Cbr/pl: 0.07). By performing scaffold hopping from this series, we observed compounds having a tetrahydrocarbazole core (**6**) exhibiting CB_1 potency and desirable physico-chemical properties (**Fig. 2**). In the present study, we report *N*-methyl-3-(tetrahydro-2*H*-pyran-4-yl)-2,3,4,9-tetrahydro-1*H*-carbazole-6-carboxamides as a novel class of hCB_1/hCB_2 dual agonists with very low CNS penetration.

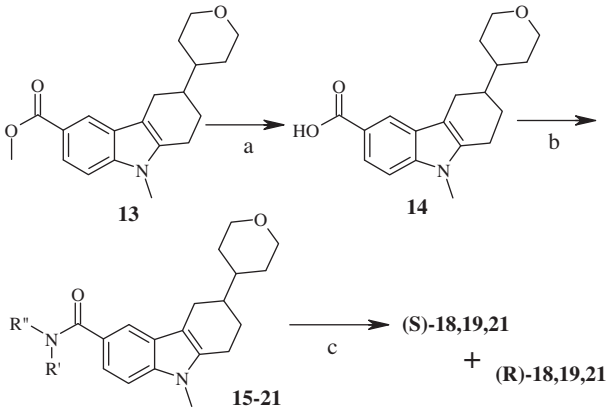

Scheme 2. Reagents and conditions: (a) NaOH, MeOH/H_2O (88%); (b) R′R″NH, HATU, DIPEA, DMF (60–90%); (c) chiral separation with ChiraPak® AD column, Hexane/EtOH (60/40).

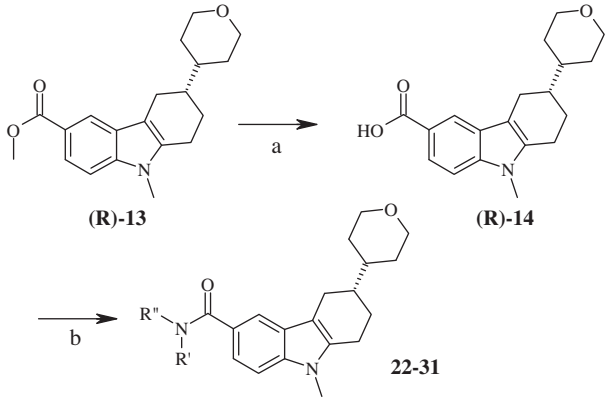

Scheme 3. Reagents and conditions: (a) LiOH, dioxane/H_2O (99%); (b) R′R″NH, HATU, DIPEA, DMF (60–90%).

The synthesis of common intermediate (**13**) is outlined in Scheme 1.[31] Commercially available or readily prepared 1-(benzyloxy)-4-bromobenzene (**7**) was treated with BuLi at −78 °C and

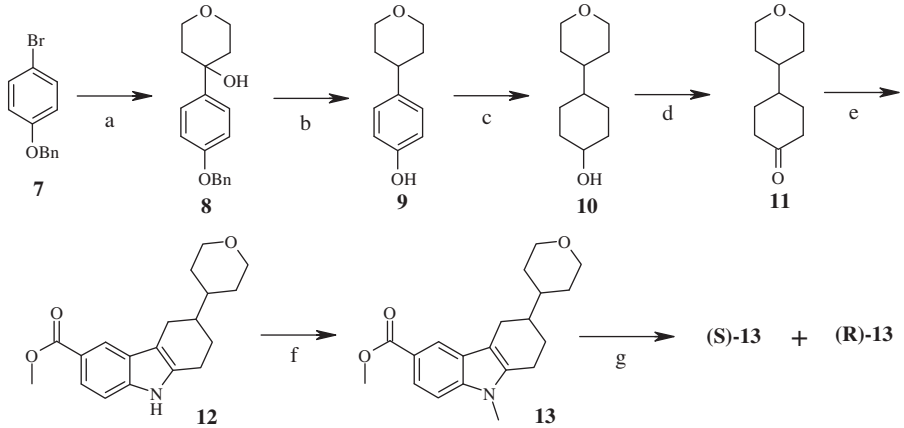

Scheme 1. Reagents and conditions: (a) (i) BuLi, THF, −78 °C; (ii) tetrahydro-4*H*-pyran-4-one (67%). (b) H_2, Pd/C, 3M HCl, THF/MeOH, (99%). (c) Rh/Al_2O_3 5%, MeOH, (100%). (d) Bleach, TEMPO, CH_2Cl_2, (88%). (e) (i) 4-Hydrazinobenzoic acid hydrochloride, HCl, dioxane; (ii) MeOH, HCl (89%). (f) NaH/MeI THF (90%); (g) ChiralCel®OD, Hexane/EtOH (60/40).

Table 1
Properties of selected *N*-methyl-3-(tetrahydro-2*H*-pyran-4-yl)-2,3,4,9-tetrahydro-1*H*-carbazole-6-carboxamides

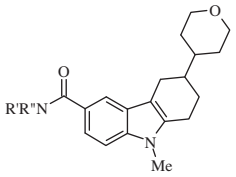

Compound	R′R″N	hCB$_1$ *Ki*[a] (nM)	hCB$_2$ *Ki*[a] (nM)	hCB$_1$ EC$_{50}$[a,b] (nM)	hClint[c] (μL/min/mg)	hERG IC$_{50}$ (μM)	Solubility[d] (μM, pH 7.4)
2		46	2	112 (100%)	nd	nd	2
4		35	19	73 (112%)	nd	nd	0
AZ599		120	9	49 (120%)	52	3.1	>1030
15	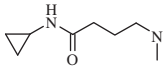	7.1	nd	16.2 (113%)	73	>33	444
16	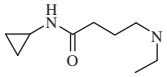	2.8	nd	2.9 (114%)	143	>33	224
17	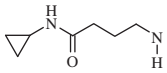	1440	nd	nd	47	>31	1
18	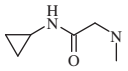	44.5	26.3	95.3 (121%)	37	>33	108
19	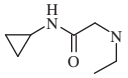	7.3	nd	6.2 (106%)	53	>33	36
20	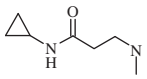	655	nd	nd	nd	>33	523
21	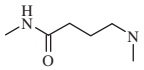	53.7	nd	78.9 (121%)	27	>33	1550

[a] Values are means of at least three measurements.
[b] E_{max} are reported in brackets.
[c] Metabolic stability performed in human liver microsomes in presence of NADPH using test compounds at 1 μM.
[d] Thermodynamic solubility measured in a pH 7.4 buffer using HPLC with UV detection for quantification; nd: not determined.

followed by addition of tetrahydro-4*H*-pyran-4-one to give 4-[4-(benzyloxy)phenyl]tetrahydro-2*H*-pyran-4-ol (**8**), which was reduced to **9** under acidic hydrogenation conditions.

4-(Tetrahydro-2*H*-pyran-4-yl)phenol was further reduced under rhodium-catalyzed hydrogenation to 4-(tetrahydro-2*H*-pyran-4-yl)cyclohexanol (**10**), which was oxidized to **11**. 4-(Tetrahydro-2*H*-pyran-4-yl)cyclohexanone was subjected to standard Fischer indole synthesis condition with 4-hydrazinobenzoic acid hydrochloride and followed by esterification to provide methyl 3-(tetrahydro-2*H*-pyran-4-yl)-2,3,4,9-tetrahydro-1*H*-carbazole-6-carboxylate (**12**). *N*-Methylation of **12** was done under basic conditions to afford the desired product **13**. Methyl 9-methyl-3-(tetrahydro-2*H*-pyran-4-yl)-2,3,4,9-tetrahydro-1*H*-carbazole-6-carboxylate was separated into its enantiomers **(R)-13** and **(S)-13**, whose configurations were established by vibrational circular dichroism (VCD)[32] and X-ray crystallography.

Synthesis of *N*-methyl-3-(tetrahydro-2*H*-pyran-4-yl)-2,3,4,9-tetrahydro-1*H*-carbazole-6-carboxamides (**15**–**21**) is outlined in Scheme 2. Compound **13** was hydrolyzed under basic conditions to 9-methyl-3-(tetrahydro-2*H*-pyran-4-yl)-2,3,4,9-tetrahydro-1*H*-carbazole-6-carboxylic acid **14**, which was subjected to amide coupling conditions using 2-(7-aza-1*H*-benzotriazole-1-yl)-1,1,3,3-tetramethyluronium hexafluorophosphate (HATU) to afford the desired amides **15**–**21.** Compounds **18**,**19** and **21** were further separated into their enantiomers **(R)**- & **(S)-18**, **(R)**- & **(S)-19**, and **(R)**- & **(S)-21**.

Synthesis of (*R*)-*N*-methyl-3-(tetrahydro-2*H*-pyran-4-yl)-2,3,4,9-tetrahydro-1*H*-carbazole-6-carboxamides (**22**–**31**) is shown in Scheme 3. **(R)-13** was hydrolyzed under basic conditions to (*R*)-9-methyl-3-(tetrahydro-2*H*-pyran-4-yl)-2,3,4,9-tetrahydro-1*H*-carbazole-6-carboxylic acid **(R)-14**, which was subjected to amide coupling conditions to afford the desired amides **22**–**31**.

During the efforts on the γ-carbolines, it was found that the incorporation of an amide moiety provided compounds with full CB$_1$ agonist potency completely devoid of affinity for the hERG potassium channel.

When this SAR was applied to the tetrahydrocarbazole series, similar effects were found on the CB$_1$ potency[33] and hERG activity. As shown in Table 1, linear chain amide derivative **15** exhibits very potent hCB$_1$ binding affinity (hCB$_1$ *Ki* = 7.1 nM) and excellent hCB$_1$ agonist activity (hCB$_1$ EC$_{50}$ = 16.2 nM) while its hERG IC$_{50}$ is over 33 μM. As compared to the *N*-methyl amide **15**, the *N*-ethyl derivative **16** is even more potent with increased hCB$_1$ EC$_{50}$ by over 5-fold. In the case of glycine amides, *N*-ethyl derivative **19** displays a 15-fold increase in hCB$_1$ EC$_{50}$ as compared to its *N*-methyl analog **18**. On the other hand, compound **17** displays very poor hCB$_1$ binding affinity, which indicates that the NH has detrimental effects on CB$_1$ potency.

Chirality plays an important role in CB$_1$ potency. Selected compounds are presented in Table 2. Racemic **21** was separated into its faster eluting (R)-enantiomer and slower eluting (S)-enantiomer by preparative chiral HPLC separation. The stereochemical assignments were established by X-ray analyses. **(S)-21** is much less active (hCB$_1$ *Ki* = 576 nM). The more potent (R)-enantiomer **(R)-21** demonstrated good hCB$_1$ full agonist activity with extremely low hERG activity. Racemates **18** & **19** were also separated by chiral

Table 2
Chirality effects on CB_1 potency

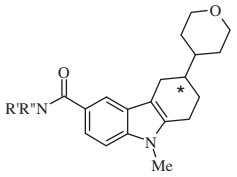

Compound	R′R″N	hCB_1 *Ki*[a] (nM)	hCB_2 *Ki*[a] (nM)	hCB_1 EC_{50}[a,b] (nM)	hClint[c] (μL/min/mg)	hERG IC_{50} (μM)	Solubility[d] (μM, pH 7.4)
(R)-18	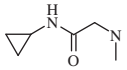	24.5	21.5	39.9 (116%)	30	>33	86
(S)-18		177	49.1	446 (111%)	38	>33	63
(R)-19	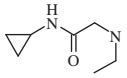	4.2	nd	1.9 (106%)	36	nd	30
(S)-19		17.3	nd	24.2 (106%)	nd	nd	49
(R)-21	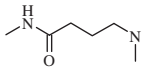	29.3	15.5	51.4 (116%)	26	105	1123
(S)-21		576	nd	nd	31	nd	1070

[a] Values are means of at least three measurements.
[b] E_{max} are reported in brackets.
[c] Metabolic stability performed in human liver microsomes in presence of NADPH using test compounds at 1 μM.
[d] Thermodynamic solubility measured in a pH 7.4 buffer using HPLC with UV detection for quantification; nd: not determined.

Table 3
Properties of (*R*)-*N*-methyl-3-(tetrahydro-2*H*-pyran-4-yl)-2,3,4,9-tetrahydro-1*H*-carbazole-6-carboxamides

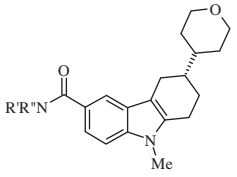

Compound	R′R″N	hCB_1 EC_{50}[a,b] (nM)	hClint[c] (μL/min/mg)	Cbr/pl	hERG IC_{50} (μM)	Caco-2[d] (10^{-6} cm/s)	Solubility[e] (μM, pH 7.4)
2		112 (100%)	nd	2.3	nd	nd	2
4		73 (112%)	nd	0.29	nd	nd	0
AZ599		49 (120%)	52	0.07	3.1	13	>1030
(R)-18	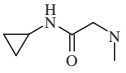	39.9 (116%)	30	0.024	>33	27	86
(R)-19	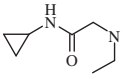	1.9 (106%)	36	0.09	nd	23	30
(R)-21	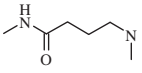	51.4 (116%)	26	0.02	>33	12	1120
22	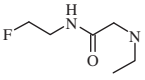	9.8 (107%)	33	0.068	nd	nd	71
23	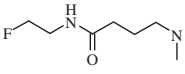	12.9 (108%)	50	0.02	nd	nd	470
24	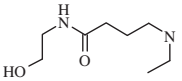	30.7 (113%)	38	<0.02	>33	nd	760
25	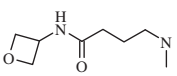	43.7 (116%)	29	0.019	>33	nd	1670
26	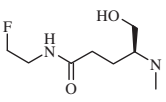	61.4 (118%)	27	0.025	>33	0.11	1310

(*continued on next page*)

Table 3 (*continued*)

Compound	R′R″N	hCB$_1$ EC$_{50}$[a,b] (nM)	hClint[c] (μL/min/mg)	Cbr/pl	hERG IC$_{50}$ (μM)	Caco-2[d] (10^{-6} cm/s)	Solubility[e] (μM, pH 7.4)
27	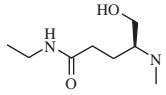	78.7 (126%)	21	0.011	>33	0.21	1930
28	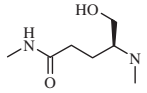	101 (124%)	15	<0.02	>33	0.15	>3000
29	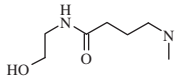	173 (120%)	17	nd	>33	nd	2490
30	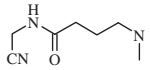	70.6 (110%)	42	nd	>33	nd	300
31	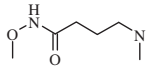	291 (104%)	36	nd	>33	nd	1330

[a] Values are means of at least three measurements.
[b] E_{max} are reported in brackets.
[c] Metabolic stability performed in human liver microsomes in presence of NADPH using test compounds at 1 μM.
[d] Transwell assay: apparent permeability (apical to basolateral) across a Caco-2 cell monolayer measured under pH gradient pH 6.5–7.4 using test compound at 10 μM applied on the apical side.
[e] Thermodynamic solubility measured in a pH 7.4 buffer using HPLC with UV detection for quantification; nd: not determined.

Table 4
Pharmacokinetic Parameters of **(R)-21** in Sprague–Dawley Rats[a]

Intravenous administration (2 μmol/kg)	
t $_{1/2}$[b]	2.4 h
VDss	0.3 L/kg
CL	2.8 mL/min/kg
Intravenous administration (9 μmol/kg)	
T_{max}	2.2 h
C_{max}	6.3 μM
F (%)	~100%

[a] Values represent the means only for $n = 3$.
[b] Terminal half-life.

HPLC. In both cases, the (R)-enantiomers display better hCB$_1$ agonist activities (hCB$_1$ EC$_{50}$) by over 10-fold as compared to the corresponding (S)-enantiomers.

Once the stereospecificity of the compounds on hCB$_1$ had been determined, efforts were focused on enantiomerically pure (R)-isomers. The selected compounds are presented in Table 3. Various groups are tolerated on the linear amide moiety, including F, MeO, CN, and hydroxyl. All the compounds tested exhibited full hCB$_1$ agonist properties with very low hERG binding affinity for the compounds tested and low CNS distributions. However, because of its overall pharmacokinetics and solubility profiles, **(R)-21** was preferred over the other analogues to be tested in vivo.

The pharmacokinetic profile of **(R)-21** after oral and intravenous administration to Sprague–Dawley rats is shown in Table 4. Oral bioavailability was excellent (~100%), indicating that pre-systemic first-pass metabolism is limited and gut permeability is not limiting. The small steady-state volume of distribution (0.3 L/kg) and moderate terminal half-life (2.4 h) after iv administration were likely due to the low systemic clearance (2.8 mL/min/kg). Combined with high affinity for plasma protein (97.9% bound), the fact that **(R)-21** is a good P-glycoprotein (Pgp) substrate (efflux ratio of 31 in MDR1-MDCK cells) resulted in a low CNS distribution as demonstrated by in vivo microdialysis studies.[34] Following oral administration of 9 μmol/kg, a C_{max} of 6.3 μM was observed at 2 h post dose.

The metabolic stability of **(R)-21** in rat and human liver microsomes was moderate (Clint: 61 and 26 μL/min/mg of microsomal protein respectively). When considering the plasma protein binding in rat and binding to microsomal incubations (as calculated by method published by Austin et al.[35]), the predicted clearance (CL) was low (3.2 mL /min/kg) and in line with the observed in vivo CL (2.8 mL/min/kg). Applying the same scaling method, the predicted clearance in human would be approximately 2 mL/min/kg, which is consistent with our expectation of an acceptable bioavailability in man. The cytochrome P$_{450}$ inhibitory potential of **(R)-21** was determined in human liver microsomes by use of the major isoforms CYP1A2, CYP2C9, CYP2C19, CYP2D6, and CYP3A4, in order to assess the potential likelihood of drug interactions. Compound **(R)-21** exhibited only moderate inhibition against CYP2C9 (IC$_{50}$ = 7 μM) and was inactive (>20 μM) against the other isoforms.

Compound (**R**)-**21** showed a dose dependant reversal of heat hyperalgesia in vivo when tested subcutaneously in the rat Carrageenan inflammatory pain model at doses of 10, 30 and 100 μmol/kg.[36] These doses resulted in total plasma concentrations of 6.9, 9.1 and 50.7 μM, while none could be detected in the brain.[37] These observations further validate that peripherally restricted cannabinoid agonists can contribute to analgesia.

In summary, we have identified a new *N*-methyl-3-(tetrahydro-2*H*-pyran-4-yl)-2,3,4,9-tetrahydro-1*H*-carbazole-6-carboxamide series as potent mixed CB$_1$/CB$_2$ agonists with good physicochemical properties and low CNS penetration. Investigations into the further development of these ligands are currently underway.

References and notes

1. Matsuda, L. A.; Lolait, S. J.; Brownstein, M. J.; Young, A. C.; Bonner, T. I. *Nature* **1990**, *346*, 561.
2. Munro, S.; Thomas, K. L.; Abushaar, M. *Nature* **1993**, *365*, 61.
3. Herkenham, M.; Lynn, A. B.; Little, M. D.; Johnson, M. R.; Melvin, L. S.; DeCosta, B. R.; Rice, K. C. *Proc. Natl. Acad. Sci. U.S.A.* **1990**, *87*, 1932.
4. Mailleux, P.; Vanderhaeghen, J. *J. Neuroscience* **1992**, *48*, 655.
5. Cabral, G. A.; Raborn, E. S.; Griffin, L.; Dennis, J.; Marciano-Cabral, F. *Br. J. Pharmacol.* **2009**, *153*, 240.
6. Ashton, J. *Curr. Opin. Investig. Drugs* **2007**, *8*, 373.
7. Svizenska, I.; Dubovy, P.; Sulcova, A. *Pharmacol. Biochem. Behav.* **2008**, *90*, 501.
8. Das, S. K.; Chakrabarti, R. *Curr. Med. Chem.* **2006**, *13*, 1429.
9. Basavarajappa, B. S. *Mini-Rev. Med. Chem.* **2007**, *7*, 769.
10. Chapman, V.; Finn, D. P. *Rev. Anal.* **2003**, *7*, 25.
11. Walter, L.; Stella, N. *Br. J. Pharmacol.* **2004**, *141*, 775.

12. Ashton, J.; Milligan, E. D. *Curr. Opin. Investig. Drugs* **2008**, *9*, 65.
13. Turcotte, D.; Le Dorze, J.-A.; Esfahani, F.; Frost, E.; Gomori, A.; Namka, M. *Expert Opin. Pharmacother.* **2010**, *11*, 17.
14. Talwar, R.; Potluri, V. K. *CNS Neurolog. Disord. Drug Targets* **2011**, *10*, 536.
15. Karst, M.; Wippermann, S.; Ahrens, J. *Drugs* **2010**, *70*, 2409.
16. Burns, T. L.; Ineck, J. R. *Ann. Pharmacother.* **2006**, *40*, 251.
17. Sellito, I.; Le Bourdonnec, B.; Worm, K.; Goodman, A.; Savolainen, M. A.; Chu, G.-H.; Ajello, C. W.; Saeui, C. T.; Leister, L. K.; Cassel, J. A.; DeHaven, R. N.; LaBuda, C. J.; Koblish, M.; Little, P. J.; Brogdon, B. L.; Smith, S. A.; Dolle, R. E. *Bioorg. Med. Chem. Lett.* **2010**, *20*, 387.
18. Gleave, R. J.; Beswick, P. J.; Brown, A. J.; Giblin, G. M. P.; Goldsmith, P.; Haslam, C. P.; Mitchell, W. L.; Nicholson, N. H.; Page, L. W.; Patel, S.; Roomans, S.; Slingsby, B. P.; Swarbrick, M. E. *Bioorg. Med. Chem. Lett.* **2010**, *20*, 465.
19. Malan, T. P., Jr.; Ibrahim, M. M.; Lai, J.; Vanderah, T. W.; Makriyannis, A.; Porreca, F. *Curr. Opin. Pharmacol.* **2003**, *3*, 62.
20. Quartiho, A.; Mata, H. P.; Ibrahim, M. M.; Vanderah, T. W.; Porreca, F.; Makriyannis, A.; Malan, T. P., Jr. *Anesthesiology* **2003**, *99*, 955.
21. Kelly, S.; Jhaveri, M. D.; Sagar, D. R.; Kendall, D. A.; Chapman, V. *Eur. J. Neurosci.* **2003**, *18*, 2239.
22. Fride, E.; Feigin, C.; Ponde, D. E.; Breuer, A.; Hanus, L.; Arshavsky, N.; Mechoulam, R. *Eur. J. Pharmacol.* **2004**, *506*, 179.
23. Dyson, A.; Peacock, M.; Chen, B.; Courade, J.-P.; Yaqoob, M.; Groarke, A.; Brain, C.; Loong, Y.; Fox, A. *Pain* **2005**, *116*, 129.
24. Richardson, J. D.; Kilo, S.; Hargreaves, K. M. *Pain* **1998**, *75*, 111.
25. Adam, J. M.; Clark, J. K.; Davies, K.; Everett, K.; Fields, R.; Francis, S.; Jeremiah, F.; Kiyoi, T.; Maidment, M.; Morrison, A.; Ratcliff, P.; Prosser, A.; Schulz, J.; Wishart, G.; Baker, J.; Boyce, S.; Campbell, R.; Cottney, J. E.; Deehan, M.; Martin, I. *Bioorg. Med. Chem. Lett.* **2012**, *22*, 2932.
26. Odan, M.; Ishizuka, N.; Hiramatsu, Y.; Inagaki, M.; Hashizume, H.; Fujii, Y.; Mitsumori, S.; Morioka, Y.; Soga, M.; Deguchi, M.; Yasui, K.; Arimura, A. *Bioorg. Med. Chem. Lett.* **2012**, *22*, 2894.
27. Rukwied, R.; Watkinson, A.; McGlone, F.; Dvorak, M. *Pain* **2003**, *102*, 283.
28. Salim, K.; Schneider, U.; Burstein, S.; Hoy, L.; Karst, M. *Neuropharmacology* **2005**, *48*, 1164.
29. Dziadulewicz, E. K.; Bevan, S. J.; Brain, C. T.; Coote, P. R.; Culshaw, A. J.; Davis, A. J.; Edwards, L. J.; Fisher, A. J.; Fox, A. J.; Gentry, C.; Groarke, A.; Hart, T. W.; Huber, W.; James, I. F.; Kesingland, A.; Vecchia, L. L.; Loong, Y.; Lyothier, I.; McNair, K.; O'Farrell, C.; Peacock, M.; Portmann, R.; Schopfer, U.; Yaqoob, M.; Zadrobilek, J. *J. Med. Chem.* **2007**, *50*, 3851.
30. Cheng, Y.-X.; Pourashraf, M.; Luo, X.; Srivastava, S.; Walpole, C.; Salois, D.; St-Onge, S.; Payza, K.; Lessard, E.; Yu, X. H.; Tomaszewski, M. *Bioorg. Med. Chem. Lett.* **2012**, *22*, 1619.
31. All products gave satisfactory analytical characterization showing purity >95% as determined by HPLC using a Zorbax C-18 column (λ = 215, 254 and 280 nm). ^{1}H NMR spectra were obtained from a 400 MHz Varian Unity Plus spectrometer. Mass spectra were obtained on a Micromass Quattro micro API or an Agilent 1100 Series LC/MSD instrument using loop injection. Selected analytical characterizations; ***Compound 5 (AZ599)***: ^{1}H NMR (METHANOL-D4) δ ppm 0.89 (d, *J* = 6.40 Hz, 3 H), 0.59–1.09 (m, 2H), 1.13 (t, *J* = 7.42 Hz, 3H), 1.47–1.76 (m, 3H), 1.77–1.89 (m, 2H), 2.08 (d, *J* = 12.29 Hz, 2H), 2.70–2.83 (m, 1H), 2.96–3.08 (m, 1H), 3.29–3.47 (m, 5H), 3.42 (q, *J* = 7.25 Hz, 2H), 3.55–3.70 (m, 2H), 3.85–4.00 (m, 1H), 4.03 (dd, *J* = 11.65, 4.48 Hz, 2H), 4.34–4.70 (m, 3H), 7.32 (d, *J* = 8.70 Hz, 1H), 7.56 (s, 1H), 7.95 (d, *J* = 8.45 Hz, 1H); $[M+H]^+$ 474.0; ***Compound (R)-13***: ^{1}H NMR (CHLOROFORM-D) δ ppm 1.42–1.50 (m, 1H) 1.50–1.57 (m, 2H) 1.58–1.67 (m, 2H) 1.76 (d, *J* = 11.72 Hz, 2H) 2.12–2.18 (m, 1H) 2.38–2.47 (m, 1H) 2.64–2.73 (m, 1H) 2.77–2.85 (m, 1H) 2.90 (dd, *J* = 16.02, 2.73 Hz, 1H) 3.42 (t, *J* = 11.72 Hz, 2H) 3.64 (s, 3H) 3.93 (s, 3H) 4.04 (dd, *J* = 10.94, 3.52 Hz, 2H) 7.24 (d, *J* = 8.59Hz, 1H) 7.86 (dd, *J* = 8.59, 1.56 Hz, 1H) 8.23 (d, *J* = 1.17 Hz, 1H); $[M+H]^+$ = 328.22; k′ = 3.20 (Chiral HPLC ChiralPak® AD, 40% ethanol/60% hexane). ***Compound (R)-21***: ^{1}H NMR (400 MHz, METHANOL-D4) δ ppm 1.37–1.50 (m, 2H) 1.52–1.61 (m, 3H) 1.77 (t, *J* = 12.70 Hz, 2H) 1.86 (s, 1H) 1.96 (s, 2H) 2.13–2.20 (m, 1H) 2.26 (s, 1H) 2.34–2.44 (m, 1H) 2.49 (s, 1H) 2.64–2.73 (m, 2H) 2.79–2.90 (m, 2H) 3.04 (s, 3H) 3.36–3.47 (m, 3H) 3.55 (s, 1H) 3.63 (s, 3H) 3.98 (dd, *J* = 10.94, 3.52 Hz, 2H) 7.13 (s, 1H) 7.31 (d, *J* = 8.20 Hz, 1H) 7.46 (s, 1H); $[M+H]^+$ = 426.2; k′ = 3.20. (Chiral HPLC ChiralPak® AD, 40% ethanol/60% hexane). ***Compound (S)-21***: ^{1}H NMR (400 MHz, METHANOL-D4) δ ppm 1.38–1.50 (m, 2H) 1.53–1.60 (m, 3H) 1.78 (t, *J* = 12.30 Hz, 2H) 1.85 (s, 1H) 1.96 (s, 2H) 2.13–2.20 (m, 1H) 2.26 (s, 1H) 2.39 (dd, *J* = 16.21, 6.84 Hz, 1H) 2.49 (s, 1H) 2.65–2.74 (m, 2H) 2.80–2.89 (m, 2H) 3.04 (s, 3H) 3.37–3.47 (m, 3H) 3.55 (s, 1H) 3.63 (s, 3H) 3.98 (dd, *J* = 11.33, 3.91 Hz, 2H) 7.12 (s, 1H) 7.31 (d, *J* = 8.59 Hz, 1H) 7.46 (s, 1H); $[M+H]^+$ = 426.2; k′ = 4.79 (Chiral HPLC ChiralPak® AD, 40% ethanol/60% hexane).
32. A Monte Carlo molecular mechanics search of low energy conformers for the R configuration of 13 was conducted using MacroModel within the Maestro graphical interface (Schrödinger Inc.). The 16 lowest energy conformers identified were used as starting points and minimized using density functional theory (DFT) within Gaussian 03. Simulations of infrared and VCD spectra for each conformer were generated using an in-house written program to fit Lorentzian line shapes (10 cm-1 line width) to the computed spectra. In this manner, direct comparisons between simulated and experimental spectra were made.
33. *Ki* values were measured by displacement of the agonist ^{3}H-CP55,940 binding on membranes of Human Embryonic Kidney (HEK) 293s stable cell lines transfected with the cloned human CB1 receptor. EC_{50} were measured by GTPγ^{35}S binding on membranes of Human Embryonic Kidney (HEK) 293 EBNA stable cell line transfected with the cloned human CB1 receptor using WIN55,212–2 (compound **2**) as the reference agonist for E_{max} calculations.
34. Lessard, E.; Schroeder, P.; Ellis, A.; Yu, X. H.; Ducharme, J. Abstracts: Clinical Pharmacology and Therapeutics IXth World Congress 2008 *Can. J. Clin. Pharmacol.* **2008**, *15*(3), e550.
35. Austin, R. P.; Barton, P.; Cockroft, S. L.; Wenlock, M. C.; Riley, R. J. *Drug Metab. Dispos.* **2002**, *30*, 1497.
36. This study was conducted under a protocol that has been approved by an ethical committee. The animals were kept and experiments were performed at our main site (AZRDM: AstraZeneca R&D Montreal) or at a site which has accreditation from: CCAC (Canadian Council on Animal Care), AAALAC (Association for the Assessment and Accreditation of Laboratory Animal Care) and/or approved by AZGVC (AstraZeneca Global Veterinary Council) for study conduct.
37. The determination of the total plasma or brain concentration of (**R**)-**21** was performed by protein precipitation (after homogenization of brain samples), followed by reversed-phase liquid chromatography and electrospray mass spectrometry. Twenty microliters of biological samples from the CNS experiments (plasma and brain) and blank matrix(ces) are added manually into a 96 well plate. All the in vivo samples are precipitated by adding 60 μL of ACN+. The plate is carefully capped, vortexed and centrifuged at 9000g for 30 min at 4 °C. The samples are then ready to be analyzed by LC-MS/MS. After preparing an analytical standard in ACN+, serial dilutions are carried out in order to prepare a calibration curve. The range of the calibration curve is 1.22 to 1000.